

A Multi-Parameter Investigation of Gravitational Slip

Scott F. Daniel*,¹ Robert R. Caldwell,¹ Asantha Cooray,² Paolo Serra,² and Alessandro Melchiorri³

¹*Department of Physics and Astronomy, Dartmouth College, Hanover, NH 03755 USA*

²*Department of Physics and Astronomy, University of California, Irvine, CA 92697 USA*

³*Physics Department and Sezione INFN, University of Rome,*

“La Sapienza,” P.le Aldo Moro 2, 00185 Rome, Italy

(Dated: October 23, 2018)

A detailed analysis of gravitational slip, a new post-general relativity cosmological parameter characterizing the degree of departure of the laws of gravitation from general relativity on cosmological scales, is presented. This phenomenological approach assumes that cosmic acceleration is due to new gravitational effects; the amount of spacetime curvature produced per unit mass is changed in such a way that a Universe containing only matter and radiation begins to accelerate as if under the influence of a cosmological constant. Changes in the law of gravitation are further manifest in the behavior of the inhomogeneous gravitational field, as reflected in the cosmic microwave background, weak lensing, and evolution of large-scale structure. The new parameter, ϖ_0 , is naively expected to be of order unity. However, a multiparameter analysis, allowing for variation of all the standard cosmological parameters, finds that $\varpi_0 = 0.09^{+0.74}_{-0.59}$ (2σ) where $\varpi_0 = 0$ corresponds to a Λ CDM universe under general relativity. Future probes of the cosmic microwave background (Planck) and large-scale structure (Euclid) may improve the limits by a factor of four.

I. INTRODUCTION

Cosmic acceleration [1, 2] can be caused by new fluids, new theories of gravity, or some admixture of both [3]. This uncertainty places a premium on descriptions of the so-called “dark physics” which remain useful across different models and in spite of varying assumptions. In the case of new fluids (dark energy), the literature chooses to speak in terms of the equation of state w and its derivative [4]. In the case of new gravitational physics, the model-independent *lingua franca* is the relationship between the Newtonian (ψ) and longitudinal (ϕ) gravitational potentials. The potentials, implicitly defined through the perturbed Robertson-Walker metric

$$ds^2 = a^2[-(1 + 2\psi)d\tau^2 + (1 - 2\phi)d\vec{x}^2], \quad (1)$$

are most familiar for their roles in Newton’s equation, $\ddot{\vec{x}} = -\vec{\nabla}\psi$, and the Poisson equation, $\nabla^2\phi = 4\pi G a^2 \delta\rho$ under general relativity (GR).

The gravitational potentials are equal in the presence of non-relativistic stress-energy under GR. Alternate theories of gravity make no such guarantee. Scalar-tensor [5, 6] and $f(R)$ theories [7, 8, 9], braneworld scenarios such as Dvali-Gabadadze-Porrati gravity [10, 11, 12], and massive gravity [13, 14] all predict a systematic difference or “slip”, so that $\phi \neq \psi$ in the presence of non-relativistic stress-energy. Efforts to develop a parametrized-post-Friedmannian (PPF) framework to phenomenologically describe this behavior are just as prolific: Refs. [15, 16, 17, 18, 19, 20, 21, 22, 23, 24] all offer parametrizations quantifying the departure from $\phi = \psi$ due to new gravitational effects. We choose to work with the parametriza-

tion proposed in Ref. [16]:

$$\psi = [1 + \varpi(z)]\phi \quad (2)$$

$$\varpi(z) = \varpi_0(1 + z)^{-3}. \quad (3)$$

We assume the existence of a theory of gravitation that leads to an expansion history that is indistinguishable from that produced by a spatially-flat, Λ CDM scenario with density parameters Ω_m and $\Omega_\Lambda = 1 - \Omega_m$. This assumption is not essential, but it allows our analysis to focus solely on PPF effects. Our naive expectation is that $\varpi \simeq \Omega_\Lambda/\Omega_m$ by today. [Note that we have changed our notation, having previously defined $\varpi(z) = \varpi_0(\Omega_\Lambda/\Omega_m)(1 + z)^{-3}$.]

The departure from GR kicks in only when the cosmic expansion begins to accelerate. Daniel *et al.* [22] (hereafter DCCM) discuss the compatibility with other parametrizations (especially that of Ref. [23]) and compare the implications of $\varpi_0 \neq 0$ to data from the Wilkinson Microwave Anisotropy Probe (WMAP) [25], the Canada-France-Hawaii Telescope Legacy Survey (CFHTLS) [26], and various galaxy surveys [27, 28, 29]. We expand upon their analysis in this work by performing a full likelihood analysis of the cosmological parameter space.

The previous work by DCCM considered the effects of modified gravity on cosmological perturbations in a one-parameter context: i.e., “how does the the new (modified gravity) parameter affect cosmological data when all other parameters are held fixed (at the WMAP 3 year maximum likelihood values)?” They used a modified version of the Boltzmann code CMBfast [30] to evaluate the effect of ϖ_0 on the cosmic microwave background (CMB) anisotropy, matter power spectrum, weak lensing convergence correlation function, and galaxy-CMB cross-correlation power spectrum. While this analysis was useful for testing for the existence of PPF effects, the results

*scott.f.daniel@dartmouth.edu

glossed over degeneracies that exist between ϖ_0 and traditional cosmological parameters. DCCM's Figure 9 already demonstrates a potential degeneracy between ϖ_0 and σ_8 . Identifying further degeneracies and more rigorously motivating the possibility of non-zero ϖ_0 requires analysis across the full cosmological parameter space.

In the following, we present the results of a likelihood analysis based on a Monte Carlo Markov chain sampling of the space of cosmological parameters. The parameters, $\{\Omega_b h^2, \Omega_c h^2, \theta, \tau_{\text{ri}}, n_s, A_s, A_{\text{SZ}}, \varpi_0\}$, are respectively the baryon density, cold dark matter density, the ratio of the sound horizon to the angular diameter distance, the optical depth to last scattering, the scalar spectral index, the amplitude of the primordial curvature perturbations, and a normalization parameter for the SZ effect. These are the standard parameters in the convention used by the publicly-available code CosmoMC [31].

We generate our Markov Chains using CosmoMC [32, 33, 34] with modules added to calculate likelihoods based on the weak lensing [35, 36] and galaxy-CMB cross-correlation spectra [37]. The CMB data and likelihood code comes from the WMAP team's 5-year release [38]. Supernova data comes from the Union data set produced by the Supernova Cosmology Project [39]. The weak lensing data comes from the CFHTLS weak lensing survey [26, 40].

To help understand our results, we present a closed system of ordinary differential equations describing the evolution of ϕ and the matter overdensity δ under $\varpi_0 \neq 0$. These results imply a correction to the Poisson equation that was neglected in DCCM. Section II presents these equations and uses them to describe the dependence of the large-angle CMB anisotropy on ϖ_0 . Section III discusses the modifications made to the public CosmoMC codes to implement Eq. (2). Section IV presents the likelihood contours found from our Markov chains. Section V makes an attempt at forecasting the results of future experiments. We conclude in Section VI.

II. EVOLUTION OF PERTURBATIONS

The procedure for evolving the matter and metric perturbations is as follows. We assume that the perturbed stress-energy tensors for all matter and radiation are conserved independently of the theory of gravitation:

$$\nabla_\mu T^{\mu\nu} = 0. \quad (4)$$

We next impose the relationship given by Eq. (2) between potentials ϕ and ψ , which upon translation into synchronous gauge implies an evolution equation for the metric variable $\alpha \equiv (\dot{h} + 6\dot{\eta})/2k^2$:

$$\dot{\alpha} = -(2 + \varpi)\mathcal{H}\alpha + (1 + \varpi)\eta - 12\pi G a^2(\bar{\rho} + \bar{p})\sigma/k^2. \quad (5)$$

Here, a dot indicates the derivative with respect to conformal time, h and η are the synchronous-gauge metric perturbations, $\mathcal{H} = \dot{a}/a$ is the conformal-time Hubble parameter, and σ is the shear in a fluid with mean density $\bar{\rho}$

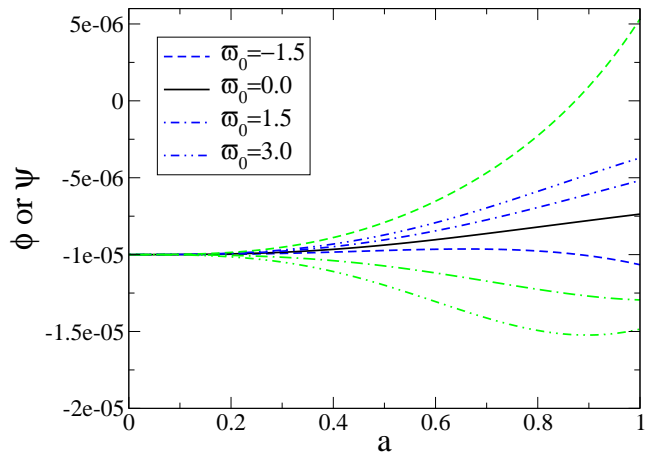


FIG. 1: The potentials ϕ and ψ are shown versus the scale factor, for different values of ϖ_0 . The blue, dark curves are ϕ , whereas the green, light curves are ψ . Note that they behave oppositely; when ϕ becomes shallower, ψ becomes deeper, and *vice versa*.

and pressure \bar{p} . (We use the same notation as Ref. [41].) We further assume that there is no preferred reference frame introduced by the new gravitational effects; there is no “dark fluid” momentum flux or velocity relative to the dark matter and baryon cosmic rest frame. This condition is imposed by enforcing the same perturbed time-space equation as in GR,

$$k^2 \dot{\eta} = 4\pi G a^2(\bar{\rho} + \bar{p})\theta, \quad (6)$$

where θ is the divergence of the velocity field in a fluid with mean density $\bar{\rho}$ and pressure \bar{p} . Satisfying this equation automatically means that Bertschinger's consistency condition, that long-wavelength curvature perturbations should evolve like separate Robertson-Walker spacetimes, is satisfied [15]. The model of $\varpi(z)$ plus the three Eqs. (4-6) close the system of equations. (See Refs. [16, 22] for further details.) In order to study the late-time behavior of the system of equations, we may neglect the shear and velocity perturbations and express the evolution equations in conformal-Newtonian/longitudinal gauge as

$$\ddot{\phi} = -(3 + \varpi)\mathcal{H}\dot{\phi} - \dot{\varpi}\mathcal{H}\phi - (1 + \varpi)(\mathcal{H}^2 + 2\dot{\mathcal{H}})\phi, \quad (7)$$

$$\dot{\delta} = 3\dot{\phi} - \left(\frac{k}{\mathcal{H}}\right)^2 \frac{\dot{\phi} + (1 + \varpi)\mathcal{H}\phi}{1 - \dot{\mathcal{H}}/\mathcal{H}^2} \quad (8)$$

where δ is the matter density contrast.

Consider the behavior of an overdense region, $\delta > 0$, as it evolves from early times when GR is valid to late times when new gravitational effects characterized by ϖ become important. At early times, when the Poisson equation is valid, $\phi < 0$ for the overdensity. While the expansion is matter-dominated, the potential remains static. However, at late times, with the onset of cosmic acceleration, the potential begins to evolve. In the case of GR, $\dot{\phi} > 0$ so the potential is stretched shallower. The density

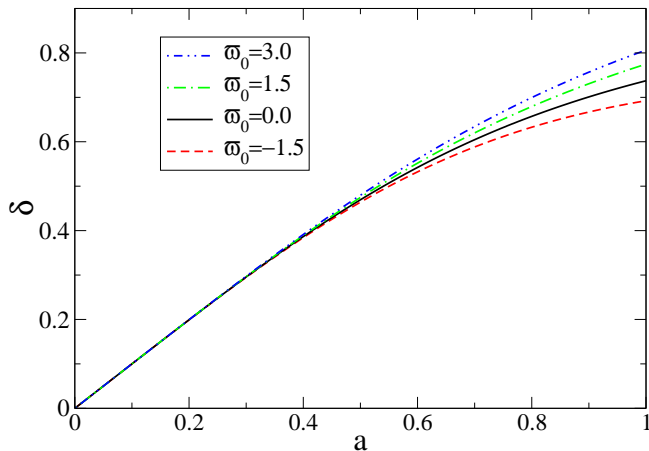


FIG. 2: The matter density contrast is shown versus the scale factor, for different values of ϖ_0 . The time evolution is obtained by integrating Eqs. (7) and (8), with initial conditions $\phi = -10^{-5}$, $\dot{\phi} = 0.0$ for $k = 0.01\text{Mpc}^{-1}$. Positive (negative) values of ϖ_0 enhance (slow) the growth of density perturbations.

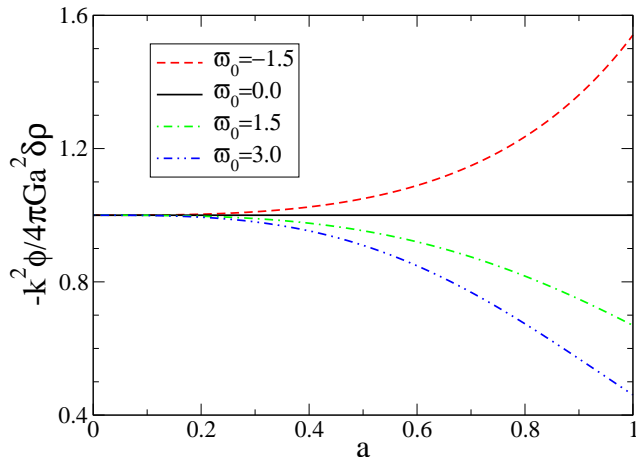


FIG. 3: The degree of deviation from the Poisson equation versus scale factor is shown for different values of ϖ_0 . Because ϖ is scale-independent, so too is the ratio $-k^2\phi/(4\pi Ga^2\delta\rho)$. For positive (negative) ϖ_0 , a given ϕ corresponds to a larger (smaller) density contrast than in GR.

contrast δ continues to grow via gravitational instability, although the rate of growth is slowed. The evolution of ϕ can be understood in terms of a competition between the expansion diluting the matter density and stretching ϕ shallower, and the accretion of matter sourcing and deepening ϕ . In GR, the accelerated expansion upsets the balance in favor of dilution, so that ϕ becomes shallower and δ grows more slowly. When $\varpi_0 \neq 0$, the competition between effects changes. Numerically integrating Eqs. (7) and (8), we find that $\varpi_0 > 0$ causes ϕ to become even shallower, yet the density contrast grows faster, as illustrated in Figs. 1 and 2. This seems counter-intuitive, since the shallower potential should provide weaker at-

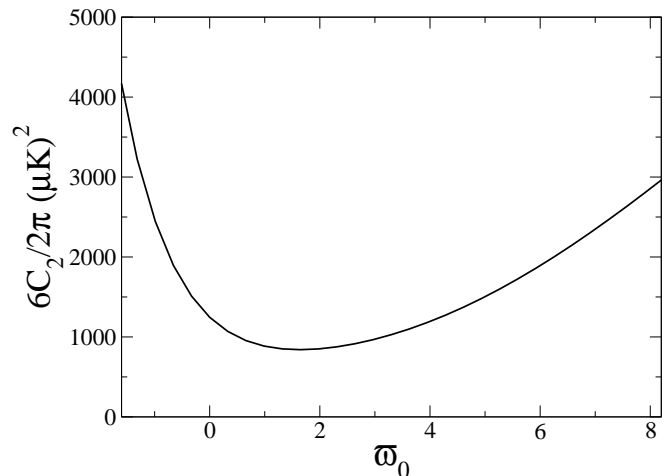


FIG. 4: The CMB quadrupole moment is shown versus ϖ_0 . As explained in the text, the quadratic dependence can be understood in terms of the influence of ϖ_0 on the ISW effect. (Reproduced from DCCM with our new normalization Eq. (3).)

traction for the accretion of surrounding matter. In the case $\varpi_0 < 0$, the potential ϕ becomes more negative or deeper, and the density contrast grows more slowly. Likewise, the deeper potential should provide greater attraction. But here the difference between ϕ and ψ is important. As seen in Fig. 1, the potential ϕ grows shallower (deeper) for $\varpi_0 > 0$ (< 0). However, the potential responsible for acceleration $\psi = (1 + \varpi)\phi$ behaves oppositely, becoming deeper (shallower). Hence, the competition swings in favor of increased clustering over dilution by the expansion.

The new behavior of ϕ and δ implies a correction to the Poisson equation. As seen in Fig. 3, for $\varpi_0 > 0$ (< 0), the density contrast grows more (less) rapidly and the potential ϕ becomes shallower (deeper), so that the ratio

$$\Gamma \equiv -k^2\phi/(4\pi Ga^2\delta\rho) \quad (9)$$

grows smaller (larger). This suggests that we can restore the Poisson equation by introducing a time-dependent gravitational constant $G_{eff} = G\Gamma$, whence $-k^2\phi = 4\pi G_{eff}a^2\delta\rho$. Note that G_{eff} is not a free function, but is determined by Eqs. (4-6). Because we have chosen ϖ to be scale-independent, G_{eff} is too. A different strategy, whereby the time- and space-dependence of G_{eff} is imposed separately [20], will not necessarily satisfy Eqs. (4-6).

We can use this new understanding to explain the curious behavior of the large-angular scale CMB anisotropy spectrum. The effect of $\varpi_0 \neq 0$ on the low l moments of the CMB anisotropy is not monotonic, as seen in Fig. 4. The cause is the suppression of the integrated Sachs-Wolfe effect (ISW) at $\varpi_0 \simeq 1$. If the gravitational potentials in the Universe are evolving with time, CMB photons will lose less (more) energy climbing out of potential wells than they gained falling in, resulting in a net

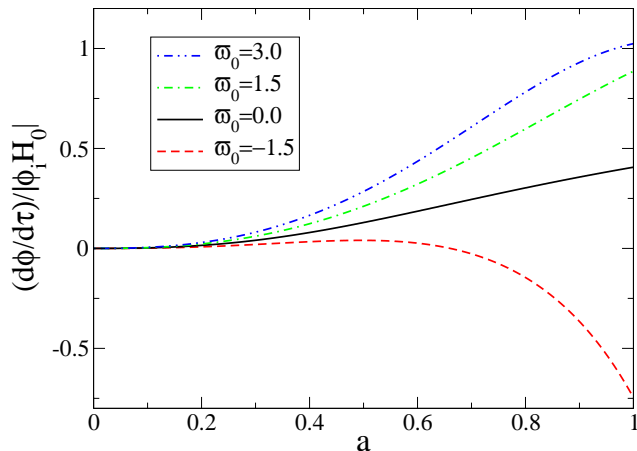


FIG. 5: The conformal time derivative of the gravitational potential ϕ is shown versus scale factor, for different values of ϖ_0 . Initial conditions are the same as in Fig. 2. The potential well is decaying when $\frac{d\phi}{d\tau}/|\phi_i H_0| > 0$, and is deepening when negative.

blue (red) shift as the potentials shrink (grow). This is the ISW effect whereby time-evolving gravitational potentials contribute to the moments of the photon distribution function, $\Theta_l(k, \eta)$, via

$$\int_0^{\tau_0} d\tau (\dot{\phi}(k, \tau) + \dot{\psi}(k, \tau)) j_l(k(\tau_0 - \tau)) \exp[-\tau_{ri}(z)]. \quad (10)$$

(See equation 8.55 of Ref. [42].) Here j_l is a spherical Bessel function of the first kind, τ is the conformal time, τ_0 is the conformal time at $z = 0$, and $\tau_{ri}(z)$ is the optical depth to redshift z . The strength of the ISW effect is determined by the sum $\dot{\phi} + \dot{\psi}$, which, using Eqs. (2-3), is given by

$$\begin{aligned} \dot{\phi} + \dot{\psi} &= \dot{\phi}(2 + \varpi) + \phi\ddot{\varpi} \\ &= \dot{\phi}(2 + \varpi) + 3\phi\mathcal{H}\varpi. \end{aligned} \quad (11)$$

Again consider the evolution of an overdensity $\delta > 0$ with $\phi < 0$. In GR, the sum is positive, $\dot{\phi} + \dot{\psi} > 0$. When $\varpi_0 < 0$, the second term in Eq. (11) is always positive. The first term is generally subdominant, since $|\dot{\phi}| < \mathcal{H}\phi$, as can be inferred from Fig. 5. Therefore $\varpi_0 < 0$ enhances the ISW effect. When $\varpi_0 > 0$, there is a competition between the first and second terms; the first term is positive, whereas the second term is negative. The first term always wins, but at some intermediate value of ϖ_0 the two terms nearly cancel, thereby suppressing the ISW effect relative to the case with $\varpi_0 = 0$. This explains the dip in the quadrupole moment versus ϖ_0 , seen in Fig. 4.

III. IMPLEMENTATION

The modifications of the Monte Carlo Markov chain software CosmoMC to allow for $\varpi_0 \neq 0$ proceed almost identically to the modifications made to CMBfast

for DCCM, with a few differences. To compare the predictions of our model with weak lensing data we adapt the weak lensing module provided by Refs. [35, 36]. We modify it to assess the likelihood in terms of the variance of the aperture mass (Eq. 5 of [26]) with a full covariance matrix [43]. Because we probe weak-lensing at non-linear scales, we calculate the power spectrum of the lensing potential by extrapolating the linear matter power spectrum P_δ to non-linear scales and using the relationship (9) between the matter overdensity δ and the gravitational potential ϕ to find the non-linear P_ϕ . Whereas CMBfast calculates the non-linear matter power spectrum from the phenomenological fit of Peacock and Dodds [44], CosmoMC (having been built around the code CAMB [33]) uses Smith *et al.*'s fit [45] (see their Appendix C). Smith *et al.* express their fit as a non-trivial function of the linear power spectrum and Ω_m . This function assumes the Λ CDM relationship between Ω_m and perturbation growth. Gravitational slip alters this relationship, as discussed above in section II. Therefore, to adapt Smith *et al.*'s fit to the case $\varpi_0 \neq 0$, we use the phenomenological relationship (DCCM equation 24)

$$\Omega_m|_{\varpi_0=0} = \Omega_m|_{\varpi_0 \neq 0} + 0.13\varpi_0 \frac{\Omega_m}{\Omega_\Lambda} \quad (12)$$

to find a $\varpi_0 = 0$, Λ CDM model with a similar growth history to our $\varpi_0 \neq 0$ model and use that value of $\Omega_m|_{\varpi_0=0}$ in Smith *et al.*'s equations (C18). Eq. (12) breaks down for $\Omega_m|_{\varpi_0 \neq 0} \leq 0.15$, but this region of parameter space is excluded to at least 2σ (see Figure 6). A second CosmoMC run with a more accurate fitting function yielded identical results to those obtained using Eq. (12).

This is not a precise method for determining the non-linear power spectrum in the presence of gravitational slip. Precision would require examination of N-body simulations which, unfortunately, implies assumptions about what alternative theory of gravity we are constraining. Recently, much work has been done attempting to calculate the non-linear power spectrum directly, without the aid of an N-body simulation. Crocce and Scoccimarro propose to expand the non-linear power spectrum as a Taylor-like sum

$$P_\delta = \sum_i P_\delta^{(i)} \quad (13)$$

where the different orders of P_δ are derived from a diagrammatic scheme similar to Feynman diagrams [46]. They find that the resulting sum (13) is much better behaved than results derived from perturbation theory (see their Figure 1). Matarrese and Pietroni [47] use the formalism of renormalization group theory to derive a generating functional for the different orders of P_δ . Taruya and Hiramatsu adapt methods from the statistical studies of fluid instabilities to separate out and solve for the cross-mode interactions in δ [48]. All of these methods yield better agreement with the results of N-body simulations than standard perturbation theory in the case of

$\varpi = 0$ (see Figure 2 of Ref. [49], Figure 8 of Ref. [47], and Figure 3 of Ref. [50]). Work has already begun adapting them to alternative gravity theories. In Ref. [51], Koyama, Taruya, and Hiramatsu extend the method of Ref. [48] to include $f(R)$ and DGP gravity theories by assuming that they can be approximated with a Brans-Dicke scalar-tensor theory on sub-horizon scales. Hiramatsu and Taruya [50] also try to encompass modified gravity theories by parametrizing them in terms of their implied effective Newton's constant $G_{\text{eff}} = \Gamma G$ (see equation 14 of the present work). Following their lead, it should be possible to adapt the non-linear power spectrum calculations of Ref. [48] – or even [46] and [47] – to account for model-independent gravitational slip. Such a calculation is beyond the scope of this work. Given the relatively well-behaved regions of parameter space allowed by experiments (see Section IV below), we do not expect this limitation to significantly influence our findings.

To incorporate the galaxy-CMB cross-correlation, we use the module written by Ho *et al.* [37]. Modifications for $\varpi_0 \neq 0$ enter as modifications to the $\phi + \psi$ power spectrum (see section II of [37]),

$$P_{\phi+\psi} = \frac{9}{4} \Omega_{m,0}^2 \left(\frac{H_0}{ck} \right)^4 \left(\frac{D_\varpi}{a} \right)^2 \left[\left(1 + \frac{1}{2} \varpi \right) \Gamma \right]^2 \times P_\delta. \quad (14)$$

Note that equation (27) of DCCM neglected the factor Γ , defined in Eq. (9), to correct the Poisson equation. The corrected weak lensing statistics show the same qualitative behavior as in Figure 10 of DCCM. However, large values $|\varpi_0| \gg 1$ have a weaker effect on the amplitude of the convergence spectrum.

IV. RESULTS

The results of our multiparameter investigation are shown in Figs. 6, 7. Fig. 6 shows the 68% and 95% contours in (Ω_m, ϖ_0) space marginalized over all other parameters. Fig. 7 shows the same contours in (σ_8, ϖ_0) space. Red (smaller) likelihood contours were generated using all available data sets (WMAP 5 year [38], Supernova Union [39], CFHTLS [26], and the galaxy surveys selected by [37]). Blue (larger) contours were generated using only the WMAP 5 year data. For each set of constraints, we generated four independent Markov Chains. We achieved convergence by running the calculations until the statistic $|1 - R|$ was much less than unity, where R is Gelman and Rubin's potential scale reduction factor, defined as the ratio of the variance across all of the chains to the mean of the variance of each individual chain evaluated for the least converged parameter. [31, 52, 53]. Our conclusions are three-fold:

- Present cosmological data constrains gravity to agree with GR, assuming a background evolution consistent with Λ CDM.

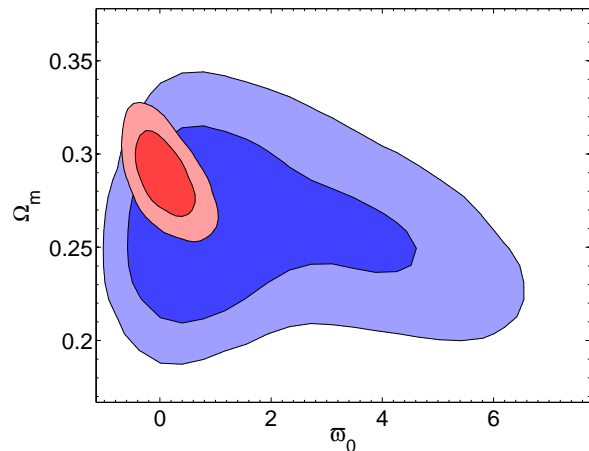


FIG. 6: The 68% and 95% likelihood contours in the $\varpi_0 - \Omega_m$ parameter space are shown. The blue contours are based on CMB data alone. The red contours add weak lensing, type Ia supernovae, and galaxy-CMB cross-correlation data.

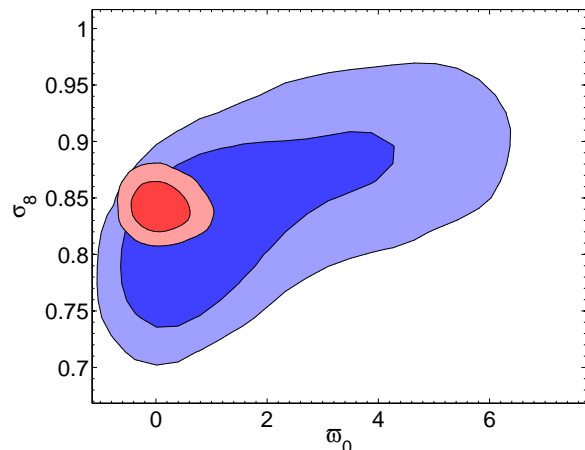


FIG. 7: The 68% and 95% likelihood contours in the $\varpi_0 - \sigma_8$ parameter space are shown. Shading is the same as in Fig. 6. Note that the addition of large-scale structure data breaks the degeneracy in $\varpi_0 - \sigma_8$.

- Very negative values of ϖ_0 are ruled out. This should not be surprising, since a sign difference between the longitudinal and Newtonian gravitational potentials would mean that test particles are repelled by overdense regions.
- Large-scale structure data (in our case, weak lensing and the galaxy-CMB correlation) are critical to constraining ϖ_0 .

The effects described in section II mean that any CMB anisotropy spectrum can be reasonably well approximated (modulo a normalization) by two possible values of ϖ_0 . DCCM Figure 1 showed that $\varpi_0 \neq 0$ has no effect on the shape of higher l multipoles within linear theory. This explains the double-peaked likelihood curve in DCCM Fig. 3 and the broad blue contours in Figs. 6

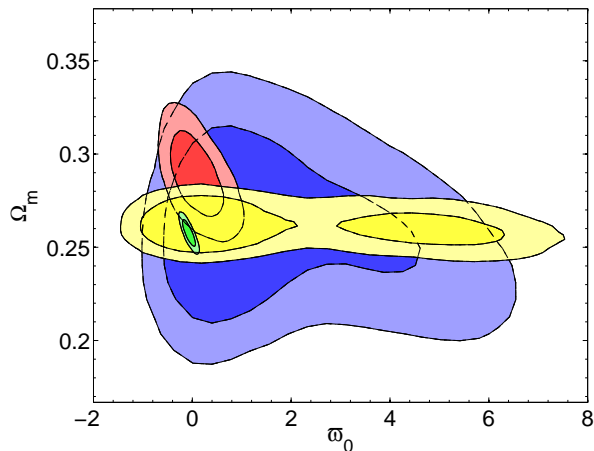


FIG. 8: The projected 68% and 95% likelihood contours in the $\varpi_0 - \Omega_m$ parameter space are shown. The yellow contours are based on mock Planck data. The green contours add mock weak lensing data. The underlying model is assumed to be $\varpi_0 = 0$ with $\Omega_m = 0.26$. The current constraints are shown for reference.

and 7 in this work. Fortunately, the effect of $\varpi_0 \neq 0$ on cosmic structure is monotonic in the range of interest (as discussed in DCCM), so that only one value of ϖ_0 is maximally likely for any given realization of weak lensing and galaxy-CMB cross-correlation data, hence the smaller red contours in Fig. 6 and 7. Marginalizing over all other parameters, the WMAP 5 year data alone gives $\varpi_0 = 1.7^{+4.0}_{-2.0}$ (2σ). Including supernovae, weak lensing, and the galaxy-CMB cross-correlation data improves the constraint to $\varpi_0 = 0.09^{+0.74}_{-0.59}$ (2σ). Table I presents the marginalized 1σ limits on the other cosmological parameters of note.

V. FORECASTS

It is useful to ask how much better our constraints will be under future experiments. We generate two mock data sets – one simulating the results of the upcoming Planck CMB experiment, the other simulating the results of a future weak lensing survey, modeled after the proposed ESA experiment Euclid – and feed them into our modified CosmoMC.

To simulate Planck data we use a fiducial model given by the best fit parameters of WMAP [38] with noise properties consistent with a combination of Planck 100-143-217 GHz channels of HFI [54]; in this case we fit also for B-modes produced by lensing of the CMB (see Ref. [55]) and we use the full-sky likelihood function given in [56].

To simulate weak lensing data, we generate a mock convergence power spectrum $P_\kappa(l)$ (equation (2) of Ref. [26]) corrected for alternative gravity as in Eq.(14). We generate data in bins of size $\Delta_l = 1$ for $2 \leq l < 100$ and $\Delta_l = 40$ for $100 < l < 2980$. We simulate the (1σ)

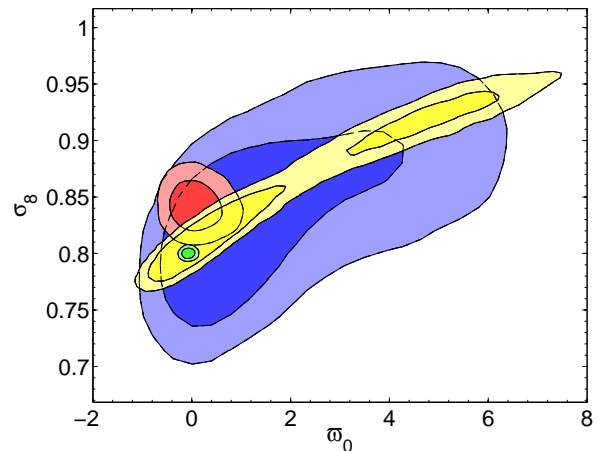


FIG. 9: The projected 68% and 95% likelihood contours in the $\varpi_0 - \sigma_8$ parameter space are shown. Shading is the same as in Fig. 8.

errors as (Eq. 11 of Ref. [57])

$$\sigma_l = \sqrt{(2/(2l+1))/(\Delta_l f_{\text{sky}})(P_\kappa(l) + \sigma_\epsilon^2/n_{\text{gal}})},$$

taking $\sigma_\epsilon = 0.25$, $n_{\text{gal}} = 35(\text{arc minute})^{-2}$ and $f_{\text{sky}} = 0.48$, consistent with values projected for ESA's Euclid experiment (Table 1 of Ref. [58]). These assumptions will give us a tighter constraint than if we had used SNAP/JDEM parameters, since SNAP/JDEM has a smaller f_{sky} by a factor of 10 [59]. We fit the redshift distribution of sources $n(z)$ from a mock data set based on Eq. 14 of Ref. [26] with parameter values taken from their Table 1. The 1σ errors in our mock $n(z)$ are reduced from actual values [43] by a factor of $1/\sqrt{2}$. The likelihood relative to the mock weak lensing data is calculated as a simple χ^2 (i.e., we assume that the covariance matrix is diagonal). This is a safe assumption according to [60]. Figs. 8 and 9 show the resulting likelihood contours.

Looking at the Planck-only (yellow) contours, we see the weakness of using CMB measurements alone to constrain ϖ_0 , as a bimodal distribution is obtained once again. We also see more clearly in Fig. 9 the degeneracy between ϖ_0 and σ_8 as normalization parameters (one can interpret the effect of ϖ_0 on δ in Fig. 2 as a renormalization of the matter power spectrum). Since weak lensing statistics depend sensitively on the power spectrum normalization, they once again break the degeneracy. Marginalizing over all other parameters, the mock datasets give the constraint $\varpi_0 = -0.07^{+0.13}_{-0.16}$ (2σ), a factor of ~ 4 improvement over the current constraint.

VI. CONCLUSIONS

If we are justified in describing the background evolution by a Λ CDM universe, then the results illustrated in Figs. 6 and 7 do not appear to indicate a significant departure from GR. In fact, these results conflict with our

parameter	$\varpi_0 \neq 0$	$\varpi_0 = 0$	WMAP 5-year
$\Omega_b h^2$	$0.02262^{+0.00059}_{-0.00058}$	$0.02264^{+0.00058}_{-0.00057}$	0.02273 ± 0.00062
$\Omega_{\text{cdm}} h^2$	0.1167 ± 0.0026	0.1170 ± 0.0016	0.1109 ± 0.0062
θ_s	$1.0417^{+0.0029}_{-0.0028}$	$1.0419^{+0.0028}_{-0.0029}$	1.0400 ± 0.0029
τ_{ri}	0.085 ± 0.016	$0.087^{+0.017}_{-0.016}$	0.087 ± 0.017
n_s	0.964 ± 0.014	0.965 ± 0.014	$0.963^{+0.014}_{-0.015}$
Ω_Λ	0.712 ± 0.014	$0.710^{+0.012}_{-0.011}$	0.742 ± 0.030
σ_8	0.842 ± 0.014	0.844 ± 0.015	0.796 ± 0.036
h	0.696 ± 0.014	0.695 ± 0.013	$0.719^{+0.026}_{-0.027}$

TABLE I: Marginalized (1σ) constraints for cosmological parameters resulting from Monte Carlo Markov chain analysis. The left and center columns are generated using all available data sets (CMB, weak lensing, supernovae, and galaxy-CMB cross-correlation). The left column is generated allows ϖ_0 to vary. The center column fixes $\varpi_0 = 0$. Because our constraint on ϖ_0 is consistent with $\varpi_0 = 0$, we find little difference between the two columns. The right column shows the constraints reported by the WMAP team in Ref. [38] based on just the WMAP 5-year data. The principal improvements from adding supernova, weak lensing, and galaxy-CMB cross-correlation data lie in constraining Ω_Λ (a result of adding the supernovae) and σ_8 (a result of adding weak lensing).

naive expectation that $\varpi_0 \simeq \Omega_\Lambda/\Omega_m$. However, these results allow the ratio of ϕ to ψ to vary by order unity from the predictions of GR at the present epoch. (Weaker constraints yet result if the redshift dependence of $\varpi(z)$ is allowed to vary; see Ref. [55].) These are not very tight constraints. As shown in Sec. V, it seems likely that experiments already under consideration will give us much tighter constraints on parametrized-post-Friedmannian departures from GR in the near future. If, indeed, future constraints improve, we may need to reconsider the assumption of homogeneous ϖ .

Throughout this paper we neglect any possible scale-dependence of ϖ . This simplifying assumption seems justified given the absence of any significant departure from GR. Were we to see evidence of a departure from GR, the onus would be on us to demonstrate the new theory’s consistency with solar system-scale tests, all of which prefer GR to one part in 10^5 (e.g. Ref. [61]). Beyond this experimental evidence, we expect that ϖ should be scale dependent simply due to the differing evolution histories of sub- and super-horizon perturbation modes. Other work has already attempted tackling this expectation. Hu and Sawicki implement a scale-dependent gravitational slip, based on the behavior seen in $f(R)$ models of gravity. [18]. Afshordi *et al.* offer a scale-dependent parametrization of $-(\psi - \phi)/(\phi + \psi)$ designed to be consistent with higher-dimensional generalizations of DGP gravity [62]. Though they find that their parametrization is capable of describing effects qualitatively consistent with tensions in current data sets, none of those tensions is strong enough to warrant a detection of alternative gravity. Koivisto

and Mota explore a different set of new gravitational effects by supposing that dark energy is an imperfect (non-zero shear) fluid [63]. Shear σ , like gravitational slip, affects the space-space, off-diagonal perturbed Einstein equation, $k^2(\phi - \psi) = 12\pi G a^2 \bar{\rho}(1 + w)\sigma$. The imperfect fluid introduces a dark flow, however, so that the gravitational effects are not fully equivalent to the results of gravitational slip. Like the present work, they find that data cannot yet definitively rule in or out the interesting regions of their parameter space. Specifically, they find that the effect of non-zero shear on the CMB anisotropy spectrum is weaker than the effect of ϖ demonstrated in DCCM.

We have also shown that the modification of the Poisson equation follows uniquely from the assumptions of our model: the enforced relationship between ϕ and ψ , stress-energy conservation, and the absence of a preferred frame indicated by a “dark flow”. This must be taken into account when conducting future tests of GR on cosmological scales.

Acknowledgments

This work was supported by NSF CAREER AST-0349213 (RC) and AST-0645427 (AC). AC and RC thank Caltech for hospitality while this work was completed. AM research is supported by ASI contract I/016/07/0 “COFIS”.

[1] A. G. Riess *et al.* [Supernova Search Team Collaboration], *Astron. J.* **116**, 1009 (1998) [arXiv:astro-ph/9805201].
[2] S. Perlmutter *et al.* [Supernova Cosmology Project Collaboration], *Astrophys. J.* **517**, 565 (1999)

[arXiv:astro-ph/9812133].
[3] J. P. Uzan, *Gen. Rel. Grav.* **39**, 307 (2007) [arXiv:astro-ph/0605313].
[4] A. Albrecht *et al.*, arXiv:astro-ph/0609591.
[5] S. M. Carroll, *San Francisco, USA: Addison-Wesley*

(2004) 513 p

- [6] C. Schmid, J. P. Uzan and A. Riazuelo, Phys. Rev. D **71**, 083512 (2005) [arXiv:astro-ph/0412120].
- [7] S. Capozziello, S. Carloni and A. Troisi, Recent Res. Dev. Astron. Astrophys. **1**, 625 (2003) [arXiv:astro-ph/0303041].
- [8] V. Acquaviva, C. Baccigalupi and F. Perrotta, Phys. Rev. D **70**, 023515 (2004) [arXiv:astro-ph/0403654].
- [9] P. Zhang, Phys. Rev. D **73**, 123504 (2006) [arXiv:astro-ph/0511218].
- [10] G. R. Dvali, G. Gabadadze and M. Porrati, Phys. Lett. B **485**, 208 (2000) [arXiv:hep-th/0005016].
- [11] A. Lue, Phys. Rept. **423**, 1 (2006) [arXiv:astro-ph/0510068].
- [12] Y. S. Song, I. Sawicki and W. Hu, Phys. Rev. D **75**, 064003 (2007) [arXiv:astro-ph/0606286].
- [13] S. L. Dubovsky, JHEP **0410**, 076 (2004) [arXiv:hep-th/0409124].
- [14] M. V. Bebronne and P. G. Tinyakov, Phys. Rev. D **76**, 084011 (2007) [arXiv:0705.1301 [astro-ph]].
- [15] E. Bertschinger, Astrophys. J. **648**, 797 (2006) [arXiv:astro-ph/0604485].
- [16] R. Caldwell, A. Cooray and A. Melchiorri, Phys. Rev. D **76**, 023507 (2007) [arXiv:astro-ph/0703375].
- [17] P. Zhang, M. Liguori, R. Bean and S. Dodelson, Phys. Rev. Lett. **99**, 141302 (2007) [arXiv:0704.1932 [astro-ph]].
- [18] W. Hu and I. Sawicki, Phys. Rev. D **76**, 104043 (2007) [arXiv:0708.1190 [astro-ph]].
- [19] L. Amendola, M. Kunz and D. Sapone, JCAP **0804**, 013 (2008) [arXiv:0704.2421 [astro-ph]].
- [20] B. Jain and P. Zhang, arXiv:0709.2375 [astro-ph].
- [21] P. Zhang, R. Bean, M. Liguori and S. Dodelson, arXiv:0809.2836 [astro-ph].
- [22] S. F. Daniel, R. R. Caldwell, A. Cooray and A. Melchiorri, Phys. Rev. D **77**, 103513 (2008) [arXiv:0802.1068 [astro-ph]]. (DCCM)
- [23] E. Bertschinger and P. Zukin, Phys. Rev. D **78**, 024015 (2008) [arXiv:0801.2431 [astro-ph]].
- [24] W. Hu, Phys. Rev. D **77**, 103524 (2008) [arXiv:0801.2433 [astro-ph]].
- [25] <http://lambda.gsfc.nasa.gov>
- [26] L. Fu *et al.*, arXiv:0712.0884 [astro-ph].
- [27] E. Gaztanaga, M. Manera and T. Multamaki, Mon. Not. Roy. Astron. Soc. **365**, 171 (2006) [arXiv:astro-ph/0407022].
- [28] T. Giannantonio *et al.*, Phys. Rev. D **74**, 063520 (2006) [arXiv:astro-ph/0607572].
- [29] A. Cabre, E. Gaztanaga, M. Manera, P. Fosalba and F. Castander, Mon. Not. Roy. Astron. Soc. Lett. **372**, L23 (2006) [arXiv:astro-ph/0603690].
- [30] U. Seljak and M. Zaldarriaga, Astrophys. J. **469**, 437 (1996) [arXiv:astro-ph/9603033].
- [31] A. Lewis and S. Bridle, <http://cosmologist.info/readme.html>
- [32] A. Lewis and S. Bridle, <http://cosmologist.info/notes/COSMOMC.ps.gz>
- [33] A. Lewis, A. Challinor and A. Lasenby, Astrophys. J. **538**, 473 (2000) [arXiv:astro-ph/9911177].
- [34] A. Lewis and S. Bridle, Phys. Rev. D **66**, 103511 (2002) [arXiv:astro-ph/0205436].
- [35] R. Massey *et al.*, arXiv:astro-ph/0701480.
- [36] J. Lesgourgues, M. Viel, M. G. Haehnelt and R. Massey, JCAP **0711**, 008 (2007) [arXiv:0705.0533 [astro-ph]].
- [37] S. Ho, C. Hirata, N. Padmanabhan, U. Seljak and N. Bahcall, Phys. Rev. D **78**, 043519 (2008) [arXiv:0801.0642 [astro-ph]].
- [38] J. Dunkley *et al.* [WMAP Collaboration], arXiv:0803.0586 [astro-ph].
- [39] M. Kowalski *et al.*, arXiv:0804.4142 [astro-ph].
- [40] M. Kilbinger *et al.*, arXiv:0810.5129 [astro-ph].
- [41] C. P. Ma and E. Bertschinger, Astrophys. J. **455**, 7 (1995) [arXiv:astro-ph/9506072].
- [42] S. Dodelson, *Amsterdam, Netherlands: Academic Pr. (2003) 440 p.*
- [43] M. Kilbinger, private communication (2008).
- [44] J. A. Peacock and S. J. Dodds, Mon. Not. Roy. Astron. Soc. **280**, L19 (1996) [arXiv:astro-ph/9603031].
- [45] R. E. Smith *et al.* [The Virgo Consortium Collaboration], Mon. Not. Roy. Astron. Soc. **341**, 1311 (2003) [arXiv:astro-ph/0207664].
- [46] M. Crocce and R. Scoccimarro, Phys. Rev. D **73**, 063519 (2006) [arXiv:astro-ph/0509418].
- [47] S. Matarrese and M. Pietroni, JCAP **0706**, 026 (2007) [arXiv:astro-ph/0703563].
- [48] A. Taruya and T. Hiramatsu, arXiv:0708.1367 [astro-ph].
- [49] M. Crocce and R. Scoccimarro, Phys. Rev. D **77**, 023533 (2008) [arXiv:0704.2783 [astro-ph]].
- [50] T. Hiramatsu and A. Taruya, arXiv:0902.3772 [astro-ph.CO].
- [51] K. Koyama, A. Taruya and T. Hiramatsu, arXiv:0902.0618 [astro-ph.CO].
- [52] A. Gelman and D. Rubin, *Statistical Science* **7**, 457 (1992).
- [53] S. P. Brooks and A. Gelman, *Journal of Computational and Graphical Statistics* **7**, 434 (1998).
- [54] Planck collaboration [arXiv:astro-ph/0604069]
- [55] P. Serra *et al.* (2009) (in preparation)
- [56] A. Lewis, Phys. Rev. D **71**, 083008 (2005) [arXiv:astro-ph/0502469].
- [57] A. R. Cooray, Astron. Astrophys. **348**, 31 (1999) [arXiv:astro-ph/9904246].
- [58] T. D. Kitcing, A. F. Heavens, L. Verde, P. Serra and A. Melchiorri, Phys. Rev. D **77**, 103008 (2008) [arXiv:0801.4565 [astro-ph]].
- [59] <http://snap.lbl.gov/>
- [60] A. Cooray and W. Hu, Astrophys. J. **554**, 56 (2001) [arXiv:astro-ph/0021087].
- [61] B. Bertotti, L. Iess and P. Tortora, Nature **425**, 374 (2003).
- [62] N. Afshordi, G. Geshnizjani and J. Khoury, arXiv:0812.2244 [astro-ph].
- [63] T. Koivisto and D. F. Mota, Phys. Rev. D **73**, 083502 (2006) [arXiv:astro-ph/0512135].